Observers for hyperbolic systems with two delays in the nonlocal boundary condition and its application

Hideki Sano[1], Jeanne Redaud[1,2]

[1] Graduate School of System Informatics, Kobe University
[2] Laboratoire des Signaux et Systemes, CentraleSupelec, Universite Paris-Saclay

1 Introduction

In recent years, many papers have reported that the backstepping method is very effective for solving stabilization problems and state estimation problems for systems of first-order hyperbolic partial differential equations [1, 2, 3, 6, 7, 8, 9]. The backstepping method is a method to determine the feedback gain or observer gain so that the original system or the error system is transferred to the asymptotically stable target system by Volterra integral transformation or Fredholm integral transformation.

This paper addresses the state estimation problem for a first-order hyperbolic system with two delays in the nonlocal boundary condition. Time delay elements included in the boundary condition can be expressed using transport equations, and an observer is constructed for the equivalent system. As a result, the observer gains can be completely determined in seven steps. Next, we focus on a first-order hyperbolic system in which integral terms including delays are added to the van der Pol type boundary condition that produces chaotic waveforms, and show that the above observer design method can be applied to this system. In addition, we mention a secure communication method for image data using it. Since the weight functions and time lags included in the introduced integral terms can be used as a common encryption key, the key space can be greatly expanded compared to previous research [10, 11, 12, 13]. In [5], the key space is expanded by a method using a neural network for a hyperbolic system with local boundary condition. Image communication is being actively researched in the current information society, and this paper, which utilizes the synchronization of chaotic system described by delayed hyperbolic PDEs, will provide one direction. Time delay systems are difficult to handle, but when used for secure communication, they have the aspect of increasing security.

2 System description

Let $\gamma_i(x)$ $(i = 1, 2)$ be real-valued functions satisfying $\gamma_i \in H^1(0, 1)$ and $\gamma_i(0) = \gamma_i(1) = 0$ and τ_i $(i = 1, 2)$ be positive numbers satisfying $0 < \tau_1 < \tau_2$. Let κ be a real constant. Consider the following first-order hyperbolic system defined on the interval $[0, 1]$, whose

boundary condition includes time lags τ_i.

$$\Sigma_0 : \begin{cases} u_t(t,x) = u_x(t,x), \quad v_t(t,x) = -v_x(t,x), \\ u(t,1) = \begin{cases} \phi_1(t) + \phi_2(t), & \text{for } 0 \le t < \tau_1, \\ \displaystyle\int_0^1 \gamma_1(x) u(t-\tau_1, x)dx + \phi_2(t), & \text{for } \tau_1 \le t < \tau_2, \\ \displaystyle\int_0^1 \gamma_1(x) u(t-\tau_1, x)dx + \int_0^1 \gamma_2(x) u(t-\tau_2, x)dx, & \text{for } \tau_2 \le t, \end{cases} \\ v(t,0) = \kappa u(t,0), \\ u(0,x) = u_0(x), \quad v(0,x) = v_0(x), \end{cases} \tag{1}$$

where $u_0, v_0 \in L^2(0,1)$, $\phi_1 \in L^2(0,\tau_1)$, and $\phi_2 \in L^2(0,\tau_2)$. For this system, we state the observer design method to estimate the state variables u, v. First, expressing the time lags included in the system by using transport equations, system (1) is equivalently written as follows:

$$\Sigma_0' : \begin{cases} u_t(t,x) = u_x(t,x), \quad v_t(t,x) = -v_x(t,x), \\ u(t,1) = w(t,0) + z(t,0), \quad v(t,0) = \kappa u(t,0), \\ u(0,x) = u_0(x), \quad v(0,x) = v_0(x), \\ w_t(t,x) = w_x(t,x), \quad z_t(t,x) = z_x(t,x), \\ w(t,\tau_1) = \displaystyle\int_0^1 \gamma_1(x) u(t,x)dx, \\ z(t,\tau_2) = \displaystyle\int_0^1 \gamma_2(x) u(t,x)dx, \\ w(0,x) = \phi_1(x), \quad z(0,x) = \phi_2(x). \end{cases} \tag{2}$$

3 Observer design

For system (2), consider the following hyperbolic system with input $v(t,1)$. This is called an observer.

$$\Sigma_1 : \begin{cases} \hat{u}_t(t,x) = \hat{u}_x(t,x) + f(x)(v(t,1) - \hat{v}(t,1)), \\ \hat{v}_t(t,x) = -\hat{v}_x(t,x) + g(x)(v(t,1) - \hat{v}(t,1)), \\ \hat{u}(t,1) = \hat{w}(t,0) + \hat{z}(t,0), \quad \hat{v}(t,0) = \kappa \hat{u}(t,0), \\ \hat{u}(0,x) = \hat{u}_0(x), \quad \hat{v}(0,x) = \hat{v}_0(x), \\ \hat{w}_t(t,x) = \hat{w}_x(t,x) + h(x)(v(t,1) - \hat{v}(t,1)), \\ \hat{z}_t(t,x) = \hat{z}_x(t,x) + i(x)(v(t,1) - \hat{v}(t,1)), \\ \hat{w}(t,\tau_1) = \displaystyle\int_0^1 \gamma_1(x) \hat{u}(t,x)dx, \\ \hat{z}(t,\tau_2) = \displaystyle\int_0^1 \gamma_2(x) \hat{u}(t,x)dx, \\ \hat{w}(0,x) = \hat{\phi}_1(x), \quad \hat{z}(0,x) = \hat{\phi}_2(x). \end{cases} \tag{3}$$

Introducing the error variables $\tilde{u} := u - \hat{u}$, $\tilde{v} := v - \hat{v}$, $\tilde{w} := w - \hat{w}$, $\tilde{z} := z - \hat{z}$, we have the error system

$$\begin{cases} \tilde{u}_t(t,x) = \tilde{u}_x(t,x) - f(x)\tilde{v}(t,1), \\ \tilde{v}_t(t,x) = -\tilde{v}_x(t,x) - g(x)\tilde{v}(t,1), \\ \tilde{u}(t,1) = \tilde{w}(t,0) + \tilde{z}(t,0), \quad \tilde{v}(t,0) = \kappa\tilde{u}(t,0), \\ \tilde{u}(0,x) = \tilde{u}_0(x), \quad \tilde{v}(0,x) = \tilde{v}_0(x), \\ \tilde{w}_t(t,x) = \tilde{w}_x(t,x) - h(x)\tilde{v}(t,1), \\ \tilde{z}_t(t,x) = \tilde{z}_x(t,x) - i(x)\tilde{v}(t,1), \\ \tilde{w}(t,\tau_1) = \displaystyle\int_0^1 \gamma_1(x)\tilde{u}(t,x)dx, \\ \tilde{z}(t,\tau_2) = \displaystyle\int_0^1 \gamma_2(x)\tilde{u}(t,x)dx, \\ \tilde{w}(0,x) = \tilde{\phi}_1(x), \quad \tilde{z}(0,x) = \tilde{\phi}_2(x). \end{cases} \tag{4}$$

Here, we use the Volterra–Fredholm integral transformation

$$\zeta(t,x) = \tilde{w}(t,x) - \int_0^1 k(x,y)\tilde{u}(t,y)dy - \int_0^1 l(x,y)\tilde{v}(t,y)dy, \tag{5}$$

$$\xi(t,x) = \tilde{z}(t,x) - \int_0^1 m(x,y)\tilde{u}(t,y)dy - \int_0^1 n(x,y)\tilde{v}(t,y)dy, \tag{6}$$

$$\eta(t,x) = \tilde{u}(t,x) - \int_0^x p(x,y)\tilde{u}(t,y)dy - \int_0^1 q(x,y)\tilde{v}(t,y)dy. \tag{7}$$

First of all, we set the domains of integral kernels k, l, m, n, p, and q as follows:

$$D_k = D_l = \{(x,y)\,;\, 0 \le x \le \tau_1, 0 \le y \le 1\},$$
$$D_m = D_n = \{(x,y)\,;\, 0 \le x \le \tau_2, 0 \le y \le 1\},$$
$$D_p = \{(x,y)\,;\, 0 \le x \le 1, 0 \le y \le x\},$$
$$D_q = \{(x,y)\,;\, 0 \le x \le 1, 0 \le y \le 1\}.$$

The problem is to determine the integral kernels k, l, m, n, p, q of (5)–(7) and the gains f, g, h, i of (4) so as to achieve $\tilde{u}(t,\cdot) \to 0$, $\tilde{v}(t,\cdot) \to 0$, $\tilde{w}(t,\cdot) \to 0$, $\tilde{z}(t,\cdot) \to 0$ as $t \to \infty$ (if possible, to determine the integral kernels and the gains such that all error variables become zero in a finite time). These can be determined using the backstepping method of partial differential equations.

Differentiating (5) and performing integration by parts, $\zeta_t(t,x) - \zeta_x(t,x)$ is calculated as

$$\begin{aligned} &\zeta_t(t,x) - \zeta_x(t,x) \\ &= \{-h(x) + l(x,1) + \int_0^1 k(x,y)f(y)dy + \int_0^1 l(x,y)g(y)dy\}\tilde{v}(t,1) \end{aligned}$$

$$-k(x,1)\{\tilde{w}(t,0)+\tilde{z}(t,0)\}+\{k(x,0)-\kappa l(x,0)\}\tilde{u}(t,0)$$
$$+\int_0^1\{k_x(x,y)+k_y(x,y)\}\tilde{u}(t,y)dy+\int_0^1\{l_x(x,y)-l_y(x,y)\}\tilde{v}(t,y)dy. \quad (8)$$

Similarly, differentiating (6) and performing integration by parts, $\xi_t(t,x)-\xi_x(t,x)$ is calculated as

$$\begin{aligned}&\xi_t(t,x)-\xi_x(t,x)\\&=\{-i(x)+n(x,1)+\int_0^1 m(x,y)f(y)dy+\int_0^1 n(x,y)g(y)dy\}\tilde{v}(t,1)\\&\quad -m(x,1)\{\tilde{w}(t,0)+\tilde{z}(t,0)\}+\{m(x,0)-\kappa n(x,0)\}\tilde{u}(t,0)\\&\quad +\int_0^1\{m_x(x,y)+m_y(x,y)\}\tilde{u}(t,y)dy+\int_0^1\{n_x(x,y)-n_y(x,y)\}\tilde{v}(t,y)dy. \quad (9)\end{aligned}$$

Further, differentiating (7) and performing integration by parts, $\eta_t(t,x)-\eta_x(t,x)$ is calculated as

$$\begin{aligned}&\eta_t(t,x)-\eta_x(t,x)\\&=\{-f(x)+q(x,1)+\int_0^x p(x,y)f(y)dy+\int_0^1 q(x,y)g(y)dy\}\tilde{v}(t,1)\\&\quad +\{p(x,0)-\kappa q(x,0)\}\tilde{u}(t,0)\\&\quad +\int_0^x\{p_x(x,y)+p_y(x,y)\}\tilde{u}(t,y)dy+\int_0^1\{q_x(x,y)-q_y(x,y)\}\tilde{v}(t,y)dy. \quad (10)\end{aligned}$$

We here note the following facts:

(i) If all the terms enclosed in $\{\cdot\}$ of the right-hand side of (8) are zero, $\zeta_t(t,x)-\zeta_x(t,x)=0$ holds for all $\tilde{u}$, $\tilde{v}$, $\tilde{w}$, $\tilde{z}$.

(ii) If all the terms enclosed in $\{\cdot\}$ of the right-hand side of (9) are zero, $\xi_t(t,x)-\xi_x(t,x)=0$ holds for all $\tilde{u}$, $\tilde{v}$, $\tilde{w}$, $\tilde{z}$.

(iii) If all the terms enclosed in $\{\cdot\}$ of the right-hand side of (10) are zero, $\eta_t(t,x)-\eta_x(t,x)=0$ holds for all $\tilde{u}$, $\tilde{v}$.

(iv) By (5), if $k(\tau_1,y)=\gamma_1(y)$ and $l(\tau_1,y)=0$ are satisfied, $\zeta(t,\tau_1)=0$ holds for all $\tilde{u}$.

(v) By (6), if $m(\tau_2,y)=\gamma_2(y)$ and $n(\tau_2,y)=0$ are satisfied, $\xi(t,\tau_2)=0$ holds for all $\tilde{u}$.

(vi) By (5)–(7), if $k(0,y)+m(0,y)=p(1,y)$ and $l(0,y)+n(0,y)=q(1,y)$ are satisfied, $\zeta(t,0)+\xi(t,0)=\eta(t,1)$ holds for all $\tilde{u}$, $\tilde{v}$.

(vii) Putting $x=0$ in (7), one has

$$\eta(t,0)=\tilde{u}(t,0)-\int_0^1 q(0,y)\tilde{v}(t,y)dy.$$

Under the condition $\gamma_i(0) = \gamma_i(1) = 0$ $(i = 1, 2)$, we sequentially determine the kernels k, l, m, n, p, q and the gains f, g, h, i as follows.

Calculation of observer gains

Step 1. Find the solution k on D_k to the hyperbolic equation

$$\begin{cases} k_x(x,y) + k_y(x,y) = 0, \\ k(x,1) = 0, \quad k(\tau_1, y) = \gamma_1(y). \end{cases} \tag{11}$$

Similarly, find the solution m on D_m to the hyperbolic equation

$$\begin{cases} m_x(x,y) + m_y(x,y) = 0, \\ m(x,1) = 0, \quad m(\tau_2, y) = \gamma_2(y). \end{cases} \tag{12}$$

Step 2. Find the solution l on D_l to the hyperbolic equation

$$\begin{cases} l_x(x,y) - l_y(x,y) = 0, \\ l(x,0) = \dfrac{1}{\kappa} k(x,0), \quad l(\tau_1, y) = 0. \end{cases} \tag{13}$$

Similarly, find the solution n on D_n to the hyperbolic equation

$$\begin{cases} n_x(x,y) - n_y(x,y) = 0, \\ n(x,0) = \dfrac{1}{\kappa} m(x,0), \quad n(\tau_2, y) = 0. \end{cases} \tag{14}$$

Step 3. Find the solution p on D_p to the hyperbolic equation

$$\begin{cases} p_x(x,y) + p_y(x,y) = 0, \\ p(1,y) = k(0,y) + m(0,y). \end{cases} \tag{15}$$

Step 4. Find the solution q on D_q to the hyperbolic equation

$$\begin{cases} q_x(x,y) - q_y(x,y) = 0, \\ q(x,0) = \dfrac{1}{\kappa} p(x,0), \quad q(1,y) = l(0,y) + n(0,y). \end{cases} \tag{16}$$

Step 5. Consider the hyperbolic system

$$\begin{cases} \tilde{v}_t(t,x) = -\tilde{v}_x(t,x) - g(x)\tilde{v}(t,1), \\ \tilde{v}(t,0) = \displaystyle\int_0^1 \kappa q(0,y)\tilde{v}(t,y)dy, \\ \tilde{v}(0,x) = \tilde{v}_0(x). \end{cases} \tag{17}$$

Then, determine $g(x)$ $(0 \le x \le 1)$ such that the solution $\tilde{v}$ becomes zero for $t \ge 1$. In fact, we can design $g(x)$ using the backstepping method of partial differential equations within this step. Specifically, it comes down to the problem of solving the following Volterra-type integral equation.

$$g(x) = r(x,1) + \int_x^1 r(x,y)g(y)dy, \tag{18}$$

where

$$r(x,y) = \kappa q(0, y-x). \tag{19}$$

Step 6. Solve the Volterra-type integral equation

$$f(x) = q(x,1) + \int_0^x p(x,y)f(y)dy + \int_0^1 q(x,y)g(y)dy \tag{20}$$

to determine $f(x)$ $(0 \le x \le 1)$.

Step 7. Calculate

$$h(x) = l(x,1) + \int_0^1 k(x,y)f(y)dy + \int_0^1 l(x,y)g(y)dy \tag{21}$$

to determine $h(x)$ $(0 \le x \le \tau_1)$. Similarly, calculate

$$i(x) = n(x,1) + \int_0^1 m(x,y)f(y)dy + \int_0^1 n(x,y)g(y)dy \tag{22}$$

to determine $i(x)$ $(0 \le x \le \tau_2)$.

Stability of error system (4)

As the target system of error system (4), consider the system

$$\begin{cases} \eta_t(t,x) = \eta_x(t,x), \\ \eta(t,1) = \zeta(t,0) + \xi(t,0), \\ \tilde{v}_t(t,x) = -\tilde{v}_x(t,x) - g(x)\tilde{v}(t,1), \\ \tilde{v}(t,0) = \kappa\eta(t,0) + \displaystyle\int_0^1 \kappa q(0,y)\tilde{v}(t,y)dy, \\ \zeta_t(t,x) = \zeta_x(t,x), \quad \zeta(t,\tau_1) = 0, \\ \xi_t(t,x) = \xi_x(t,x), \quad \xi(t,\tau_2) = 0. \end{cases} \tag{23}$$

In system (23), it is easy to see that $\zeta(t,\cdot)$ and $\xi(t,\cdot)$ vanish at $t = \tau_1$, $t = \tau_2$, respectively. Therefore, by $0 < \tau_1 < \tau_2$, $\eta(t,\cdot)$ vanishes at $t = \tau_2 + 1$, and $\tilde{v}$ does at $t = \tau_2 + 2$. That is, $\tilde{u}(t,\cdot)$, $\tilde{v}(t,\cdot)$, $\tilde{w}(t,\cdot)$, and $\tilde{z}(t,\cdot)$ become zero for $t \ge \tau_2 + 2$. In this way, all the error variables become zero in finite time. Actually, this is a very convenient property when designing a secure communication system.

4 Application of chaotic synchronization

4.1 Image communication

Assume that $\gamma_i(x)$, τ_i $(i = 1, 2)$ satisfy the same conditions as in Section 2. Let κ be a real constant. Consider the following first-order hyperbolic system defined on the interval $[0, 1]$.

$$\Sigma_2 : \begin{cases} u_t(t,x) = u_x(t,x), \quad v_t(t,x) = -v_x(t,x), \\ u(t,1) = \begin{cases} F_{\alpha,\beta}(v(t,1)) + \phi_1(t) + \phi_2(t), & \text{for } 0 \le t < \tau_1, \\ F_{\alpha,\beta}(v(t,1)) + \displaystyle\int_0^1 \gamma_1(x)u(t-\tau_1,x)dx + \phi_2(t), & \text{for } \tau_1 \le t < \tau_2, \\ F_{\alpha,\beta}(v(t,1)) + \displaystyle\int_0^1 \gamma_1(x)u(t-\tau_1,x)dx + \int_0^1 \gamma_2(x)u(t-\tau_2,x)dx, \\ \text{for } \tau_2 \le t, \end{cases} \\ v(t,0) = \kappa u(t,0), \\ u(0,x) = u_0(x), \quad v(0,x) = v_0(x), \end{cases} \tag{24}$$

where $u_0, v_0 \in L^2(0,1)$, $\phi_1 \in L^2(0,\tau_1)$, and $\phi_2 \in L^2(0,\tau_2)$. The relation $u = F_{\alpha,\beta}(v)$ is implicitly defined by

$$\beta(u-v)^3 + (1-\alpha)(u-v) + 2v = 0. \tag{25}$$

For the cubic equation (25), given any $v \in \mathbf{R}$, there exists a unique $u \in \mathbf{R}$ when $0 < \alpha \le 1$, $\beta > 0$ [4].

The system whose boundary condition of u at $x = 1$ of system (24) is replaced by

$$u(t,1) = F_{\alpha,\beta}(v(t,1)) \tag{26}$$

has been introduced in [4], and it is shown that, for some values of α, β, and κ, the solution (u, v) behaves chaotically. Also, an observer with $v(t, 1)$ as an input has been given in [12], and a secure communication method for image data is proposed based on Ushio's result [14, 15].

Furthermore, the system whose boundary condition of u at $x = 1$ of system (24) is replaced by

$$u(t,1) = F_{\alpha,\beta}(v(t,1)) + \int_0^1 \gamma(x)u(t,x)dx \tag{27}$$

has been introduced in [11], and an observer with $v(t, 1)$ as an input is designed using the backstepping method. It is also applied to the secure communication of image data using the same method as [12]. The weight function $\gamma(x)$ in the integral term of equation (27) is the common encryption key for secure communication. Unlike α, β, and κ, it is a function on $[0, 1]$, so the key length is long and security is enhanced. However, there is only one weight function.

For system (24), an observer whose input is $v(t, 1)$ can be constructed by the method described in Section 3. First, expressing the time lags included in the system by using transport equations, system (24) is equivalently written as follows:

$$
\Sigma_2' : \begin{cases}
u_t(t,x) = u_x(t,x), \quad v_t(t,x) = -v_x(t,x), \\
u(t,1) = F_{\alpha,\beta}(v(t,1)) + w(t,0) + z(t,0), \quad v(t,0) = \kappa u(t,0), \\
u(0,x) = u_0(x), \quad v(0,x) = v_0(x), \\
w_t(t,x) = w_x(t,x), \quad z_t(t,x) = z_x(t,x), \\
w(t,\tau_1) = \displaystyle\int_0^1 \gamma_1(x) u(t,x) dx, \\
z(t,\tau_2) = \displaystyle\int_0^1 \gamma_2(x) u(t,x) dx, \\
w(0,x) = \phi_1(x), \quad z(0,x) = \phi_2(x).
\end{cases} \tag{28}
$$

For system (28), consider the following system with input $v(t,1)$.

$$
\Sigma_3 : \begin{cases}
\hat{u}_t(t,x) = \hat{u}_x(t,x) + f(x)(v(t,1) - \hat{v}(t,1)), \\
\hat{v}_t(t,x) = -\hat{v}_x(t,x) + g(x)(v(t,1) - \hat{v}(t,1)), \\
\hat{u}(t,1) = F_{\alpha,\beta}(v(t,1)) + \hat{w}(t,0) + \hat{z}(t,0), \quad \hat{v}(t,0) = \kappa \hat{u}(t,0), \\
\hat{u}(0,x) = \hat{u}_0(x), \quad \hat{v}(0,x) = \hat{v}_0(x), \\
\hat{w}_t(t,x) = \hat{w}_x(t,x) + h(x)(v(t,1) - \hat{v}(t,1)), \\
\hat{z}_t(t,x) = \hat{z}_x(t,x) + i(x)(v(t,1) - \hat{v}(t,1)), \\
\hat{w}(t,\tau_1) = \displaystyle\int_0^1 \gamma_1(x) \hat{u}(t,x) dx, \\
\hat{z}(t,\tau_2) = \displaystyle\int_0^1 \gamma_2(x) \hat{u}(t,x) dx, \\
\hat{w}(0,x) = \hat{\phi}_1(x), \quad \hat{z}(0,x) = \hat{\phi}_2(x).
\end{cases} \tag{29}
$$

Introducing the variables $\tilde{u} := u - \hat{u}$, $\tilde{v} := v - \hat{v}$, $\tilde{w} := w - \hat{w}$, $\tilde{z} := z - \hat{z}$, we have the same error system as in (4). Therefore, an observer with input $v(t,1)$ can be actually constructed. Hence, it can be applied to secure communication of image data. In this case, the common encryption keys other than α, β, κ are $\gamma_i(x)$ and τ_i $(i = 1, 2)$, and the key space is greatly expanded, and security is enhanced. Figure 1 is a block diagram for the purpose of encrypting and transmitting image data from subsystem S_1 to subsystem S_2. In this figure, by using Σ_2' as the chaotic system and Σ_3 as the synchronizing system, secure communication of image data can be performed. Note that the vectors obtained by discretizing $u(t,x)$, $v(t,x)$, $\hat{u}(t,x)$, $\hat{v}(t,x)$ in the spatial and temporal directions are $\boldsymbol{u}[k]$, $\boldsymbol{v}[k]$, $\hat{\boldsymbol{u}}[k]$, $\hat{\boldsymbol{v}}[k]$. Also, the value obtained by discretizing $v(t,1)$ is $v_L[k]$.

4.2 Numerical simulation

In the numerical simulation, we performed the same discretization as in [10, 11, 12] for the first-order hyperbolic system.

- A monochrome image of 145×305 pixel (i.e., $M = 144$, $L = 304$) is used. The size of L determines the mesh width for space division when solving PDEs.

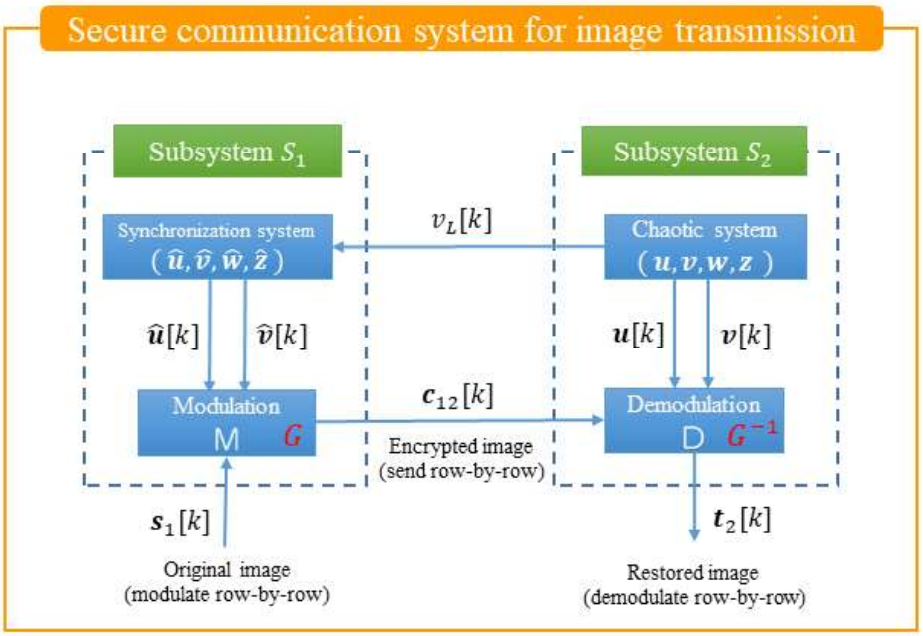

Figure 1: Secure communication system.

- In chaotic system (u, v, w, z), set $\gamma_1(x) = x(1-x)$, $\gamma_2(x) = 0.5\sin(\pi x)$, $\tau_1 = 0.5$, $\tau_2 = 2.5$, $\alpha = 0.5$, $\beta = 1$, $\kappa = (1+\mu)/(1-\mu)$, where $\mu = 0.525$. These are all common encryption keys.

When finding the observer gains, the Volterra-type integral equations are solved using the successive approximation method. In Figure 2, the thick blue solid lines are the final observer gains, which are set as $g(x) = g_4(x)$, $f(x) = f_4^4(x)$, $h(x) = h_4^4(x)$, $i(x) = i_4^4(x)$ in the simulation.

Figure 3 shows the time evolution of the L^2-norm of the solution of the error system when the proposed nonlinear observer is attached to the chaotic system. It can be seen that the L^2-norm of all error variables becomes zero after $\tau_2+2 = 4.5$. As initial conditions, we set $u_0(x) = 0.05\,x$, $v_0(x) = -0.05\,x$, $\phi_1(x) = 0.03\,x$, $\phi_2(x) = -0.03\,x$, $\hat{u}_0(x) \equiv 0$, $\hat{v}_0(x) \equiv 0$, $\hat{\phi}_1(x) \equiv 0$, $\hat{\phi}_2(x) \equiv 0$.

Figure 4 shows the numerical simulation result for secure communication of an image using the same modulation and demodulation units as in [10, 11, 12]. The runup time is from $k = 0$ steps ($t = 0$) to $k = 13680$ steps ($t = 45$), where the runup time is the time required for the waveform to reach a fully randomized chaotic state. The feature of this method is that the image to be transmitted is set in the system after the runup time has elapsed. Let the value of black be 0 and that of white be 0.01. Then, the maximum of error between the original image $\{\boldsymbol{s}_1[k]\}$ and the restored image $\{\boldsymbol{t}_2[k]\}$ was on the order of 10^{-17}. In Figure 4, the original image cannot be seen at all from the encrypted image $\{\boldsymbol{c}_{12}[k]\}$.

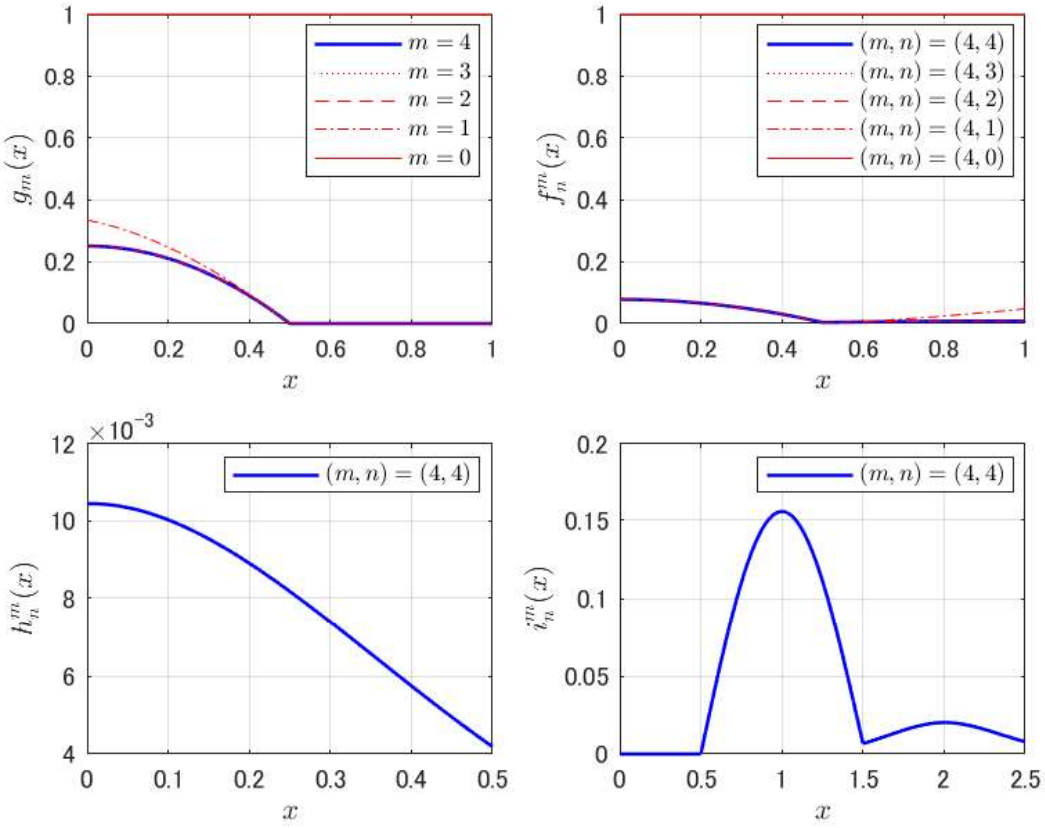

Figure 2: Observer gains for chaotic system.

5 Conclusion

In this paper, we first provided an observer design method for a first-order linear hyperbolic system with two time lags in the nonlocal boundary condition. Assuming a Luenberger type observer, the observer gains were determined using PDE backstepping. Next, we considered a chaotic system in which a nonlinear term that generates chaotic vibrations was added to the nonlocal boundary condition, and showed that an observer can be similarly designed for the nonlinear hyperbolic system. Since the designed observer works as a chaotic synchronization system in which the error system settles in a finite time, it can be applied to a secure communication system for image data, and the accuracy of the restored image was confirmed through numerical simulation. The proposed method has the advantage of expanding the key space compared to previous studies.

Acknowledgments

The Japan Society of the Promotion of Sciences (JSPS) KAKENHI Grant Number JP 21K03370 supports this research. This work was conducted during the Postdoctoral short-

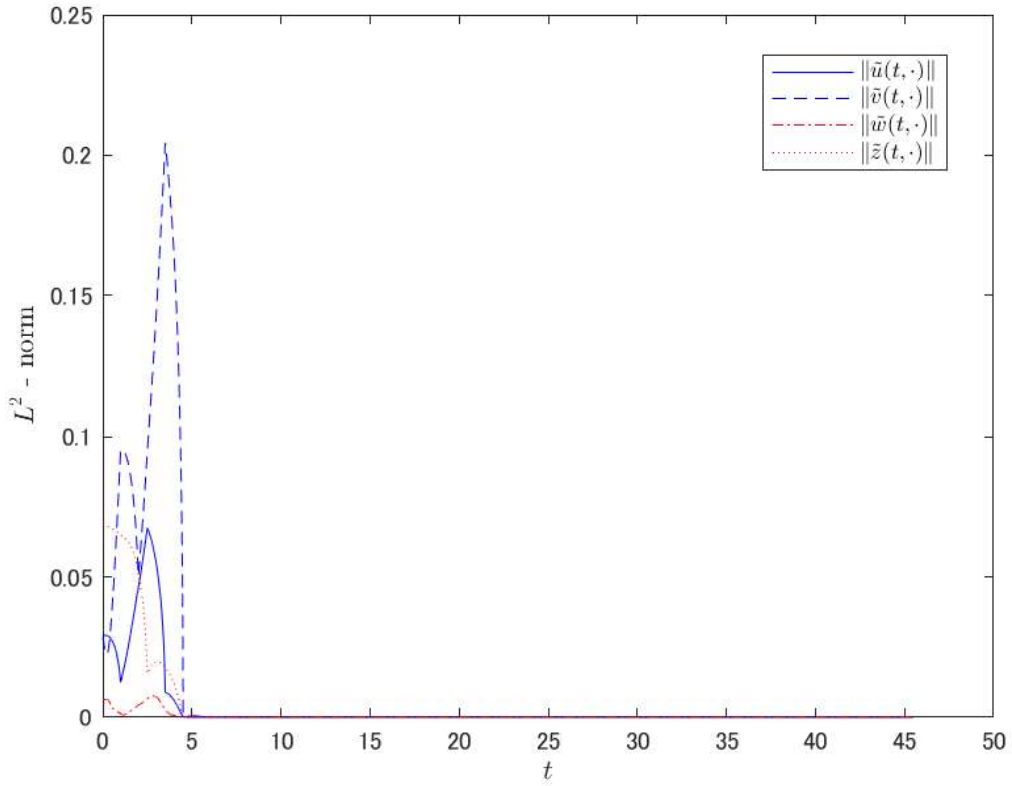

Figure 3: L^2-norm of error variables.

term fellowship (PE23006) supported by the JSPS.

References

[1] J. Auriol and F. Di Meglio. Minimum time control of heterodirectional linear coupled hyperbolic PDEs. *Automatica*, 71: 300–307, 2016.

[2] J. Auriol and F. Di Meglio. Two-sided boundary stabilization of heterodirectional linear coupled hyperbolic PDEs. *IEEE Trans. Automatic Control*, 63(8): 2421–2436, 2018.

[3] F. Bribiesca-Argomedo and M. Krstic. Backstepping-forwarding control and observation for hyperbolic PDEs with Fredholm integrals. *IEEE Trans. Automatic Control*, 60(8): 2145–2160, 2015.

[4] G. Chen, S.B. Hsu, and J. Zhou. Chaotic vibration of the wave equation with nonlinear feedback boundary control: progress and open questions. In G.R. Chen and X. Yu, editors, *Chaos Control – Theory and Applications*, LNCIS 292, pages 25–50. Springer-Verlag, Berlin, 2003.

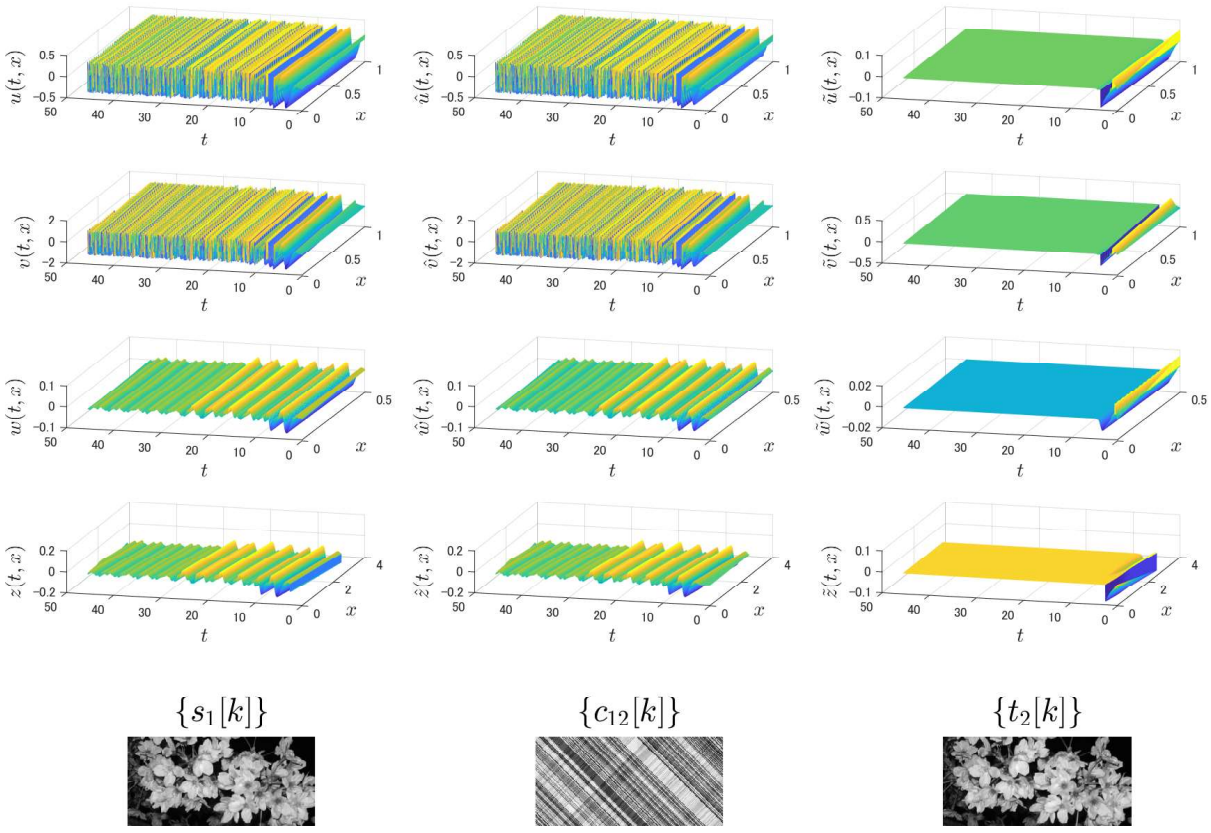

Figure 4: Image communication. $\{\boldsymbol{s}_1[k]\}$: original image. $\{\boldsymbol{c}_{12}[k]\}$: encrypted image. $\{\boldsymbol{t}_2[k]\}$: restored image.

[5] Y. Chen, H. Sano, M. Wakaiki, and T. Yaguchi. Secret communication systems using chaotic wave equations with neural network boundary conditions. *Entropy*, 23: paper no. 904, 2021.

[6] F. Di Meglio, R. Vazquez, and M. Krstic. Stabilization of a system of $n+1$ coupled first-order hyperbolic linear PDEs with a single boundary input. *IEEE Trans. Automatic Control*, 58(12): 3097–3111, 2013.

[7] L. Hu, F. Di Meglio, R. Vazquez, and M. Krstic. Control of homodirectional and general heterodirectional linear coupled hyperbolic PDEs. *IEEE Trans. Automatic Control*, 61(11): 3301–3314, 2016.

[8] J. Redaud, J. Auriol, and S.-I. Niculescu. Stabilizing output-feedback control law for hyperbolic systems using a Fredholm transformation. *IEEE Trans. Automatic Control*, 67(12): 6651–6666, 2022.

[9] H. Sano. Observers for 2×2 hyperbolic systems with coupled nonlocal boundary condition. *Proceedings of the 13th Asian Control Conference*, pages 1250–1255, 2022.

[10] H. Sano. Common encryption key generation and secure communication using PDE chaotic synchronization. *Preprints of the 22nd IFAC World Congress*, pages 10674–10679, 2023.

[11] H. Sano and M. Wakaiki. Synchronizing chaotic PDE system using backstepping and its application to image encryption. *SICE J. Control, Measurement, and System Integration*, 15(2): 182–190, 2022.

[12] H. Sano, M. Wakaiki, and T. Yaguchi. Secure communication systems using distributed parameter chaotic synchronization. *SICE Trans.*, 57(2): 78–85, 2021, (in Japanese).

[13] H. Sano, M. Wakaiki, and T. Yaguchi. Secure communication systems based on synchronization of chaotic vibration of wave equations. *J. Signal Processing*, 26(6): 147–158, 2022.

[14] T. Ushio. Chaotically synchronizing control and its application to secure communication. *Trans. Inf. Process. Soc. Jpn*, 36: 525–530, 1995, (in Japanese).

[15] T. Ushio. Control of chaotic synchronization in composite systems with applications to secure communication systems. *IEEE Trans. Circuits Syst. I: Fundamental Theory and Applications*, 43: 500–503, 1996.

Department of Applied Mathematics
Graduate School of System Informatics
Kobe University
Kobe 657-8501
JAPAN
E-mail address: `sano@crystal.kobe-u.ac.jp`